ELSEVIER

Contents lists available at ScienceDirect

Journal of Biomechanics

journal homepage: www.elsevier.com/locate/jbiomech





A theoretical framework for mechanics of diaphragm

Yi-chao Chen a,*, Aladin M. Boriek b

- a Department of Mechanical Engineering, University of Houston, Houston, TX 77204, United States of America
- ^b Department of Medicine, Baylor College of Medicine, Houston, TX 77030, United States of America

ARTICLE INFO

Keywords:
Diaphragm mechanics
Muscle activation
Anisotropic material surfaces
Diaphragm shape and stresses

ABSTRACT

A theoretical framework is developed for mechanics of the diaphragm. The diaphragm is modeled as an anisotropic elastic material surface with activation functionality. A constitutive function is formulated that relates the stresses in the diaphragm to the surface deformation gradient, the anisotropy vector, and the muscle activation parameter. The equilibrium equations for the diaphragm are derived to determine the deformed shape of the diaphragm in the process of respiration with the associated transdiaphragmatic pressures. A numerical solution is presented, that demonstrates the capability of the model to recover the experimental observations and to predict the shape and stresses of the diaphragm.

1. Introduction

The diaphragm, which is the main muscle of inspiration, consists of a curved thin muscular sheet that separates the abdominal cavity from the thoracic cavity. As for other living tissues (see Fung (1981)), the principles of mechanics can be used to study the diaphragm shape, the diaphragm stress, the transdiaphragmatic pressure, the diaphragm muscle shortening, the volume displacement, and their relations.

There have been considerable in vitro and in vivo experimental efforts to study the constitutive relations of the diaphragm, as well as the dynamic behavior of the diaphragm during spontaneous ventilation.

Kim et al. (1976) studied the diaphragmatic force–length relation and estimated the diaphragmatic tension from the transdiaphragmatic pressure. They found that the diaphragm's effective radius of curvature changes little at large lung volumes. Strumpt, Humphrey, and Yin (Strumpt et al., 1993) studied biaxial stress–strain relations of canine diaphragm in the passive state and during tetanic contraction. They reported highly nonlinear stress–strain relations, limits of extensibility, and marked anisotropy in the passive state. They concluded that "the different passive and tetanized stress–strain relations imply that different forms of constitutive laws must be used to describe passive and active muscle." Boriek et al. (2000) studied biaxial stress–strain relations of the passive canine diaphragm for different combinations of strains in the directions along and perpendicular to the muscle fibers. They found that the compliance in the transverse direction is larger than previously believed.

Boriek et al. (2005) studied the shape and tension distribution of the active canine diaphragm, by measuring transdiaphragmatic pressure and the in vivo diaphragm shape, and computing the tension Much research efforts are needed to acquire a complete understanding of the mechanical properties of the diaphragm, and to develop mechanical models to analyze and predict the shape and motion of the diaphragm in the respiration process.

- The existing investigations of the mechanical properties of the diaphragm have been based on biaxial experiments in which the principal stresses are in the direction and the transverse direction of the muscle fibers. Such experiments, while providing important information, are not sufficient to determine the constitutive function of an anisotropic material surface by which the diaphragm is modeled.
- Diaphragm muscle contraction is essential for its inspiratory action on the rib cage. The current understanding of the muscle contraction in relation to the constitutive behavior of the diaphragm is limited. The existing investigations are confined to the constitutive function of the passive diaphragm or to a separate constitutive function of the fully activated diaphragm. A comprehensive and unified constitutive function that would give the stress–strain relations in the entire range of muscle activation is currently unavailable.

distribution in the diaphragm using a finite element program. They showed that the tensions were non-uniform in the diaphragm. Greybeck et al. (2011) studied the diaphragm curvature, muscle shortening, and volume displacement during spontaneous breathing and during phrenic nerve stimulation. They reported that at maximum stimulation the muscle shortening causes a nonlinear increase in diaphragm volume displacement, concomitant with a nonlinear change in diaphragm curvature.

^{*} Corresponding author.

E-mail address: chen@uh.edu (Y.-c. Chen).

• The power of a theoretical model for diaphragm lies in its ability to predict both the shape changes and stress distribution in the diaphragm in response to normal respiration as well as higher level of ventilatory demand. While there are some isolated efforts to use finite element analysis to compute the stresses in the diaphragm from the measured diaphragm shapes, such efforts did not solve the equilibrium equations and did not fully utilize the prediction power of the mechanics theory.

This work is to fill these gaps by developing a theoretical framework for mechanics of the diaphragm. We establish a constitutive theory for the diaphragm by modeling it as an active anisotropic elastic material surface with an activation parameter and a unit vector along the muscle fibers. The diaphragm can be activated by motor units within the skeletal muscle fibers, which induces the fiber contraction, as well as alternations of stresses when the diaphragm is constrained. Based on this physical model, an elastic energy function is derived which depends on the deformation gradient and the activation parameter. It leads to the stress–strain relations from the passive to the maximum activation of the diaphragm muscles, including intermediate and submaximal activations.

The equilibrium equations are derived for general material surfaces, and are specialized to the diaphragm. The solutions of the equilibrium equations lead to the shape and stresses of diaphragm for given values of the activation parameter and the transdiaphragmatic pressure. The equations of equilibrium, which are nonlinear partial differential equations in two dimensions, can reduce to ordinary differential equations for axisymmetric deformations. Analytical/numerical solutions of the equilibrium equations are obtained to give complete descriptions of the deformation and stresses in the diaphragm for various values of the activation parameter and the transdiaphragmatic pressure.

2. Basic formulae

2.1. Kinematics

In continuum mechanics, a three-dimensional continuum that is small in one dimension is modeled as a material surface — a two-dimensional body that at any instant occupies a geometric surface in Euclidean space of dimension three. In this work, we model the diaphragm as a material surface which, in a reference configuration, occupies a domed-shaped surface \mathcal{R} . This should be regarded as an idealization, since the diaphragm has a finite thickness and is embodied with a complex structure, consisting of muscle fibers, blood vessels, connective tissues, and collagenous membranes on both the abdominal and thoracic surfaces. The idealization of material surface makes it possible to develop a concise and mathematically amenable theory for the diaphragm.

The material surface can change its shape under the actions of forces and certain activation mechanisms. This change of shape is fully described by the deformations of the material particles in the surface, which can be expressed by a mapping $\hat{\mathbf{x}}$ from \mathcal{R} to the three-dimensional space. Let the position vector of a material particle in the reference configuration \mathcal{R} be denoted by \mathbf{X} . The position vector \mathbf{x} of the material particle after deformation is

$$x = \hat{x}(X). \tag{1}$$

We denote by S the deformed surface:

$$S = \hat{\mathbf{x}}(R). \tag{2}$$

The local deformations of the material particles within a material surface element can be described by the surface deformation gradient F of \hat{x} :

$$F = \operatorname{Grad} \hat{\mathbf{x}}. \tag{3}$$

The deformation gradient as defined in (3) is a linear transformation (tensor) from the tangent space of the reference surface $\mathcal R$ to the tangent space of the deformed surface $\mathcal S$, and can be represented by a 2×2 matrix with respect to appropriate coordinate systems in the tangent spaces of $\mathcal R$ and $\mathcal S$.

2.2. Stresses

The internal distributed forces within the material surface is described by a stress vector field. Consider a cross section (an incision) of the surface S. The stress vector t is the force per unit length over the cross section. There is a stress tensor field T(x), also called the Cauchy stress tensor field, such that the stress vector t(x) at the material particle x on the cross section is given by

$$t(x) = T(x)n(x), \tag{4}$$

where n(x) is the unit outward vector that is normal to the cross section at x and is tangent to the deformed surface.

It is often convenient to use the Piola-Kirchhoff stress tensor S, which is related to the Cauchy stress tensor T through

$$S = (\det F)TF^{-T}. (5)$$

Corresponding to a cross section of the deformed surface S is a cross section of the reference surface R. Let N(X) be the unit outward vector normal to the cross section of R. The vector

$$s = SN \tag{6}$$

gives the force over the cross section of $\mathcal S$ per unit length of the cross section of $\mathcal R$. That is,

$$s dL = t dl, (7)$$

where dL is a line element over the cross section of \mathcal{R} , and dl the corresponding line element over the cross section of \mathcal{S} . Vector s is called traction vector, or engineering stress vector.

2.3. Constitutive relations

A constitutive function relates the stress in the material surface to its deformation and other state variables. For a pure elastic material surface, the Piola–Kirchhoff stress tensor is given by

$$S = \frac{\partial W(F)}{\partial F},\tag{8}$$

where W(F) is an elastic energy function whose value gives the elastic energy in the surface per unit reference area. The form of the elastic energy function can be obtained from experiments in which the deformation gradient F and the work of the stress are measured.

For an active elastic material surface, by which the diaphragm is modeled in this work, the elastic energy function depends on an additional variable η , called activation parameter:

$$W = \tilde{W}(F, \eta). \tag{9}$$

The activation parameter η , taking values between 0 and 1, describes the degree of activation. The diaphragm is in passive state when $\eta=0$, and is fully activated when $\eta=1$.

While the elastic energy function (9) represents the most general constitutive function for an active elastic material surface, determination of $\tilde{W}(F,\eta)$ for diaphragm through experiments is prohibitively difficult. On one hand, to determine the dependence of \tilde{W} on the deformation gradient F requires well-controlled experiments that subject the diaphragm to all possible deformations, which can be achieved only in vitro. On the other hand, to determine the dependence of \tilde{W} on the activation parameter η requires experiments for the diaphragm to be in various stages of activation, which can be achieved only in vivo. To determine $\tilde{W}(F,\eta)$ in the entire product space of F and η is much more difficult.

Toward overcoming these difficulties, we propose a special form of elastic energy function, which is based on the basic mechanisms of activation for skeletal muscle fibers. A major advantage of the proposed form of the elastic energy is that $\tilde{W}(F,\eta)$ can be determined from $\tilde{W}(F,0)$. That is, the constitutive function of the activated diaphragm can be determined from its constitutive function in the passive state.

A basic functional unit of skeletal muscle, called motor unit, consists of a motor neuron and a group of skeletal muscle fibers. Each muscle fiber is composed of hundreds of myofibrils containing the proteins actin and myosin. An individual myofibril is comprised of small regions called sarcomeres, each about 2 μm long in the passive state, which contain parallel-running myosin filaments and actin filaments. During the activation process, impulses are generated by the motor neuron and travel to each sarcomere, causing two opposing actin filaments to slide toward each other over the myosin, shortening the sarcomere, and therefore shortening the whole myofibril and muscle fiber. This activation mechanism suggests a decomposition of the deformation gradient ${\it F}$ as

$$F = F_e A(\eta), \tag{10}$$

where ${\bf A}(\eta)$ is an activation tensor that gives the change of diaphragm geometry due to activation, and ${\cal F}_e$ is elastic deformation gradient of the activated diaphragm. Upon activation, an unconstrained diaphragm undergoes a deformation characterized by ${\bf A}(\eta)$. Based on the activation mechanism of the skeletal muscles, we propose the following constitutive relation for the diaphragm:

$$S(F,\eta) = \frac{\partial W(F_e)}{\partial F_e} \bigg|_{F_e = FA^{-1}(\eta)},\tag{11}$$

where W is the elastic energy function of the diaphragm in its passive state, that is, $W(F) = \tilde{W}(F,0)$. The basic premise of the constitutive relations (11) is that in various activated states, the intrinsic mechanical properties of the material surface remain unchanged. Specifically, during the activation process of skeletal muscle fibers, the length of a sarcomere decreases due to the sliding of actin filaments while the composition of the sarcomere remains unaltered. The effect of activation amounts to shifting the reference configuration of the material surface to a new configuration described by $A(\eta)$.

An immediate observation is that the constitutive relation (11) allows one to determine the stress–strain relation of the diaphragm at any activated state from the stress–strain relation of the passive diaphragm, which can be obtained from an in vitro experiment, and therefore eliminates the need of conducting in vivo experiments to find the stress–strain relation of the active diaphragm. The form of the activation tensor $A(\eta)$ can be either postulated from the mechanisms of the muscle fiber activation, or deduced from the experiments of the unconstrained diaphragm in various activation states via tetanic stimulations.

2.4. Anisotropy

Since the diaphragm is composed of skeletal muscle fibers, the mechanical response of the diaphragm to loads is orientation dependent. Such an anisotropy leads to a reduced form of the elastic energy function, which depends on the deformation gradient through certain invariants under the material symmetry group actions. The theory of material symmetry for three-dimensional (bulk) materials is well developed, with the reduced elastic energy functions for various anisotropies being reported in the literature (See, for example, Ogden (1984)). However, the theory of material symmetry and reduced elastic energy functions for two-dimensional material surfaces, especially for active material surfaces, seem unavailable in the open literature. Here, we present the relevant results for diaphragm which possesses the anisotropy induced by one family of muscle fibers.

Let M(X) be a unit vector that represents the direction of a muscle fiber at the point X in the reference configuration. The direction of

the muscle fiber after an unconstrained activation is given by the unit vector

$$m = \frac{A(\eta)M}{|A(\eta)M|}. (12)$$

For the anisotropic material surface after which the diaphragm is modeled, the elastic energy function $W(F_e)$ can be written as a function of three scalar variables associated with the elastic deformation gradient:

$$W(F_e) = \hat{W}(I_1(F_e), I_2(F_e), I_3(F_e)), \tag{13}$$

where

$$I_1(F_e) = F_e \cdot F_e, \quad I_2(F_e) = (\det F_e)^2, \quad I_3(F_e) = |F_e m|^2.$$
 (14)

By (13) and (14), the derivative of the elastic energy with respect to the elastic deformation gradient F_e is found to be

$$\frac{\partial W(F_e)}{\partial F_e} = 2\hat{W}_1 F_e + 2I_2 \hat{W}_2 F_e^{-T} + 2\hat{W}_3 F_e m \otimes m, \tag{15}$$

where

$$\hat{W}_i = \frac{\partial \hat{W}}{\partial I_i}, \quad i = 1, 2, 3. \tag{16}$$

Substituting (15) into (11) gives the Piola-Kirchhoff stress tensor for the active, anisotropic material surface

$$S(F, \eta) = 2(\hat{W}_1 F A^{-1} + I_2 \hat{W}_2 F^{-T} A^T + \hat{W}_3 F A^{-1} \mathbf{m} \otimes \mathbf{m}), \tag{17}$$

the derivatives of \hat{W} are evaluated at

$$I_1 = |FA^{-1}|^2$$
, $I_2 = (\det F)^2 (\det A)^{-2}$, $I_3 = |FA^{-1}m|^2$. (18)

Consistent with the activation mechanism and the particular anisotropy of the diaphragm, we propose the following form of the activation tensor:

$$\mathbf{A}(\eta) = \mathbf{I} - \epsilon \eta \mathbf{M} \otimes \mathbf{M},\tag{19}$$

where I is the identity tensor in the tangent space of \mathcal{R} , and ϵ is a constant corresponding to the contraction strain in the fiber direction at the maximum activation under zero stress. The form of the activation tensor (19) is based on the premise that during the activation, the unconstrained material surface contracts in the direction of fiber, with no deformation in the transverse direction of the fiber. Indeed, the activation tensor (19) represents a strain $-\epsilon \eta$ in the fiber direction, and zero strain in the transverse direction.

2.5. Determination of the constitutive functions. Biaxial experiments

The theory developed in the present work enables us to determine and predict the shape, stresses, and other important characteristics of the diaphragm during the respiration process by solving an appropriate boundary value problem of the equilibrium equations. Doing so requires the form of the constitutive functions, specifically, the elastic energy function \hat{W} in (13). To our knowledge, currently there are not complete experimental data, either for animal diaphragm or for human diaphragm, to determine the elastic energy function \hat{W} . However, there is considerable amount of data acquired from biaxial experiments with loadings in and perpendicular to the muscle fiber directions. Such experiments provide partial and useful information for the constitutive function.

In the biaxial experiments of the diaphragm reported in Strumpt et al. (1993) and Boriek et al. (2000), a square diaphragm sample was excised along and transverse the muscle fibers. The sample was subjected to two sets of orthogonal forces, and the corresponding

 $^{^1}$ Since diaphragm in vivo is always constrained, the maximum contraction strain ϵ can be measured in an in vitro experiment with a stress-free diaphragm sample activated through tetanic stimulations.

stretches were measured. In a Cartesian coordinate system of which the x_1 -axis is in the direction of the fiber and x_2 -axis in the transverse direction, the deformation gradient F and the anisotropy vector M can be written in the component form

$$\boldsymbol{F} = \begin{bmatrix} \lambda_1 & 0 \\ 0 & \lambda_2 \end{bmatrix}, \quad \boldsymbol{M} = \begin{bmatrix} 1 \\ 0 \end{bmatrix}, \tag{20}$$

where λ_1 and λ_2 are the principal stretches, respectively, in the direction and the transverse direction of the fibers. Substituting (12) and (20) into (17) gives the Piola–Kirchhoff stress in the passive diaphragm in the biaxial experiment:

$$S(F,0) = 2(\hat{W}_1 F + I_2 \hat{W}_2 F^{-T} + \hat{W}_3 F M \otimes M)$$

$$= \begin{bmatrix} 2(\lambda_1 \hat{W}_1 + \lambda_1 \lambda_2^2 \hat{W}_2 + \lambda_1 \hat{W}_3) & 0\\ 0 & 2(\lambda_2 \hat{W}_1 + \lambda_1^2 \lambda_2 \hat{W}_2) \end{bmatrix},$$
(21)

where the derivatives of \hat{W} are evaluated at

$$(I_1, I_2, I_3) = (\lambda_1^2 + \lambda_2^2, \lambda_1^2 \lambda_2^2, \lambda_1^2). \tag{22}$$

In the biaxial experiment, the principal stresses, denoted by S_1 and S_2 , are obtained by dividing the force over an edge by the length of the edge before deformation. It follows from (21) that S_1 and S_2 are related to the constitutive function \hat{W} by

$$\begin{split} S_1(\lambda_1,\lambda_2) &= 2[\lambda_1 \hat{W}_1(\lambda_1^2 + \lambda_2^2, \lambda_1^2 \lambda_2^2, \lambda_1^2) + \lambda_1 \lambda_2^2 \hat{W}_2(\lambda_1^2 + \lambda_2^2, \lambda_1^2 \lambda_2^2, \lambda_1^2) \\ &\quad + \lambda_1 \hat{W}_3(\lambda_1^2 + \lambda_2^2, \lambda_1^2 \lambda_2^2, \lambda_1^2)] \end{split} \tag{23}$$

and

$$S_2(\lambda_1, \lambda_2) = 2[\lambda_2 \hat{W}_1(\lambda_1^2 + \lambda_2^2, \lambda_1^2 \lambda_2^2, \lambda_1^2) + \lambda_1^2 \lambda_2 \hat{W}_2(\lambda_1^2 + \lambda_2^2, \lambda_1^2 \lambda_2^2, \lambda_1^2)].$$
 (24)

Once S_1 and S_2 are obtained from the experiment, Eqs. (23) and (24) can be integrated to determine the energy function \hat{W} on a subset of its domain defined by (22). To find \hat{W} in its entire domain, additional experiments are needed, such as a shear experiment, or a biaxial experiment in which the edges of the square sample are not in the direction and transverse direction of the muscle fibers.

Although the biaxial experiments reported in the literature are not sufficient to determine the elastic energy function \hat{W} for the diaphragm, they provide partial and important information for the constitutive relation of the diaphragm. As we shall see, the principal stress–principal stretch relations $S_1(\lambda_1,\lambda_2)$ and $S_2(\lambda_1,\lambda_2)$ obtained from the biaxial experiments are sufficient for finding the axisymmetric solutions of the equilibrium equations.

2.6. Equations of equilibrium

A problem of great theoretical and practical importance in the diaphragm mechanics is to analytically determine and predict the shape and motion of the diaphragm and the stress distribution in the diaphragm during the process of respiration. This problem is unsolved to date, and is one of the primary motivations of the present work.

The problem can be solved by finding the solution of the equilibrium equations, which for a material surface can be written as

$$\operatorname{div} T + b = 0, (25)$$

where div is the surface divergence operator in the deformed surface, and b is the body force per unit area on the deformed surface. The transdiaphragmatic pressures across the diaphragm can be treated as a part of the body force.

By (5), the equations of equilibrium can be written in terms of the Piola–Kirchhoff stress tensor S as

$$Div S + (\det F)b = 0, (26)$$

where Div is the surface divergence operator in the reference configuration \mathcal{R} . The equations of equilibrium (26) are a system of nonlinear partial differential equations for the deformation vector x(X). The solution of the system gives the deformation vector, and therefore the shape of the diaphragm. Moreover, substituting the gradient of the deformation vector into (11) gives the stress distribution in the diaphragm.

3. Axisymmetric deformations. Reduced equations of equilibrium

The solution of the full equations of equilibrium (26) requires the constitutive function \hat{W} which is currently unavailable. Moreover, solving nonlinear partial differential equations (26) is a difficult task. In this section, we present an analysis for axisymmetric deformations, which effectively reduce (26) to a system of ordinary differential equations, and require only partial information of \hat{W} , which is obtainable from the existing biaxial experiments.

Consider a diaphragm that is axisymmetric in the reference configuration \mathcal{R} , which can be generated by rotating a planar curve about an axis. We employ the standard cylindrical coordinate system (r,θ,z) with unit base vectors e_r,e_θ , and e_z . The reference configuration \mathcal{R} can be represented by

$$X(s,\theta) = \bar{f}(s)e_r(\theta) + \bar{g}(s)e_r, \quad 0 \le s \le L, \ 0 \le \theta < 2\pi, \tag{27}$$

where \bar{f} and \bar{g} are the parametric form of the generating curve, s is the arc-length parameter, and L is the length of the generating curve. If the generating curve corresponds to a muscle fiber in the diaphragm, L is the length of the muscle fiber. The tangent space of $\mathcal R$ is spanned by two orthonormal vectors

$$E_1 = \frac{\partial X}{\partial s} / \left| \frac{\partial X}{\partial s} \right| = \bar{f}' e_r + \bar{g}' e_z$$
 and $E_2 = \frac{\partial X}{\partial \theta} / \left| \frac{\partial X}{\partial \theta} \right| = e_\theta$. (28)

Here and henceforth, a prime denotes the derivative with respect to the parameter s.

We assume that the muscle fibers in the diaphragm are in the meridian direction. The unit vector M in the fiber direction is given by

$$\mathbf{M} = \frac{\partial \mathbf{X}}{\partial s} / \left| \frac{\partial \mathbf{X}}{\partial s} \right| = E_1. \tag{29}$$

By (19) and (29), the activation tensor is

$$\mathbf{A} = (1 - \epsilon \eta) \mathbf{E}_1 \otimes \mathbf{E}_1 + \mathbf{E}_2 \otimes \mathbf{E}_2. \tag{30}$$

If the diaphragm is bonded on a circular frame and is subjected to the transdiaphragmatic pressures, a material particle moves in the plane spanned by e_r and e_z . These actions give rise to axisymmetric deformations of the diaphragm, which can be expressed by

$$\mathbf{x}(s,\theta) = f(s)\mathbf{e}_r(\theta) + g(s)\mathbf{e}_r. \tag{31}$$

The functions f and g in (31) give the generating curve of the deformed surface S, and hence the shape of the deformed diaphragm.

The tangent space of the deformed surface S is spanned by two orthonormal vectors

orthonormal vectors
$$e_1 = \frac{\partial \mathbf{x}}{\partial s} / \left| \frac{\partial \mathbf{x}}{\partial s} \right| = \frac{f' e_r + g' e_z}{\sqrt{f'^2 + g'^2}} \quad \text{and} \quad e_2 = \frac{\partial \mathbf{x}}{\partial \theta} / \left| \frac{\partial \mathbf{x}}{\partial \theta} \right| = e_{\theta}. \quad (32)$$

The deformation gradient is given by

$$F = \frac{\partial \mathbf{x}}{\partial s} \otimes \frac{\partial \mathbf{X}}{\partial s} / \left| \frac{\partial \mathbf{X}}{\partial s} \right|^2 + \frac{\partial \mathbf{x}}{\partial \theta} \otimes \frac{\partial \mathbf{X}}{\partial \theta} / \left| \frac{\partial \mathbf{X}}{\partial \theta} \right|^2 = \sqrt{f'^2 + g'^2} e_1 \otimes E_1 + \frac{f}{f} e_2 \otimes E_2.$$
(33)

It follows from (10), (30), and (33) that

$$F_{e} = FA^{-1} = \frac{\sqrt{f'^{2} + g'^{2}}}{1 - \epsilon \eta} e_{1} \otimes E_{1} + \frac{f}{\bar{f}} e_{2} \otimes E_{2}. \tag{34}$$

Also, (12) and (19) give

$$m = \frac{(I - \epsilon \eta M \otimes M)M}{|(I - \epsilon \eta M \otimes M)M|} = M. \tag{35}$$

Substituting (19), (29), (34), and (35) into (14) gives

$$I_1 = \frac{f'^2 + g'^2}{(1 - \epsilon \eta)^2} + \frac{f^2}{\bar{f}^2}, \quad I_2 = \frac{f^2(f'^2 + g'^2)}{\bar{f}^2(1 - \epsilon \eta)^2}, \quad I_3 = \frac{f'^2 + g'^2}{(1 - \epsilon \eta)^2}.$$
 (36)

Furthermore, substituting (29), (34), (35), and (36) into (17) gives the Piola–Kirchhoff stress tensor

$$S = S_{11}e_1 \otimes E_1 + S_{22}e_2 \otimes E_2, \tag{37}$$

where

$$S_{11} = \frac{2\sqrt{f'^2 + g'^2}}{1 - \epsilon \eta} \Big(\hat{W}_1 + \frac{f^2}{\bar{f}^2} \hat{W}_2 + \hat{W}_3 \Big), \quad S_{22} = \frac{2f}{\bar{f}} \Big[\hat{W}_1 + \frac{f'^2 + g'^2}{(1 - \epsilon \eta)^2} \hat{W}_2 \Big].$$
(38)

By (28), (32), (37), and (38), the surface divergence of the Piola-Kirchhoff stress tensor S is found to be

$$\operatorname{Div} \mathbf{S} = \frac{\partial \mathbf{S}}{\partial s} \frac{\partial \mathbf{X}}{\partial s} / \left| \frac{\partial \mathbf{X}}{\partial s} \right|^2 + \frac{\partial \mathbf{S}}{\partial \theta} \frac{\partial \mathbf{X}}{\partial \theta} / \left| \frac{\partial \mathbf{X}}{\partial \theta} \right|^2$$

$$= \frac{1}{f} \left[\frac{\bar{f} S_{11}(f' e_r + g' e_z)}{\sqrt{f'^2 + g'^2}} \right]' - \frac{S_{22}}{\bar{f}} e_r. \tag{39}$$

The diaphragm is subjected to esophageal pressure P_{es} on the upper surface and to gastric pressure P_{ga} on the lower surface. The transdiaphragmatic pressure P is defined by

$$P = P_{ga} - P_{es}. (40)$$

The transdiaphragmatic pressure can be treated as a body force applied on the diaphragm:

$$b = Pe_2 \times e_1. \tag{41}$$

By (32), (33), (39), and (41), the equilibrium equations (26) become

$$\frac{1}{\bar{f}} \left[\frac{\bar{f} S_{11}(f'e_r + g'e_z)}{\sqrt{f'^2 + g'^2}} \right]' - \frac{S_{22}}{\bar{f}} e_r - \frac{Pf}{\bar{f}} (f'e_z - g'e_r) = \mathbf{0}, \tag{42}$$

which give two ordinary differential equations for f and g:

$$\left(\frac{\bar{f}f'S_{11}}{\sqrt{f'^2+g'^2}}\right)' - S_{22} + Pfg' = 0, \quad \left(\frac{\bar{f}g'S_{11}}{\sqrt{f'^2+g'^2}}\right)' - Pff' = 0. \tag{43}$$

Integrating (43)₂ yields

$$\frac{\bar{f}g'S_{11}}{\sqrt{f'^2 + g'^2}} - \frac{1}{2}Pf^2 = c,\tag{44}$$

where the constant of integration c can be determined by appropriate boundary conditions. By (44), Eq. (43), can be written as

$$\left[\frac{(c+\frac{1}{2}Pf^2)f'}{g'}\right]' - S_{22} + Pfg' = 0.$$
 (45)

Since the stress components S_{11} and S_{22} given by (38) involve the constitutive function \hat{W} , it may seem that solving the equilibrium equations (44) and (45) would require the function form of \hat{W} , which is currently unavailable in the literature. However, by comparing (23) and (24) to (38), as well as (22) to (36), we find that S_{11} and S_{22} in (44) and (45) are identical, respectively, to the principal stresses S_1 and S_2 in (23) and (24), that are obtained from a biaxial experiment. Thus, the equilibrium equations can be rewritten as

$$\left[\frac{(c+\frac{1}{2}Pf^2)f'}{g'}\right]' - S_2(\lambda_1, \lambda_2) + Pfg' = 0, \qquad \frac{\bar{f}g'S_1(\lambda_1, \lambda_2)}{\sqrt{f'^2 + g'^2}} - \frac{1}{2}Pf^2 = c,$$
(46)

where

$$\lambda_1 = \frac{\sqrt{f'^2 + g'^2}}{1 - \epsilon n} \quad \text{and} \quad \lambda_2 = \frac{f}{\bar{f}}. \tag{47}$$

The axisymmetric deformations (31) have effectively reduced the equilibrium equations (26) to ordinary differential equations, which greatly facilitates the numerical or analytical solutions. Moreover, only the principal stress–principal stretch relations from the existing biaxial experiments are needed for the reduced equilibrium equations.

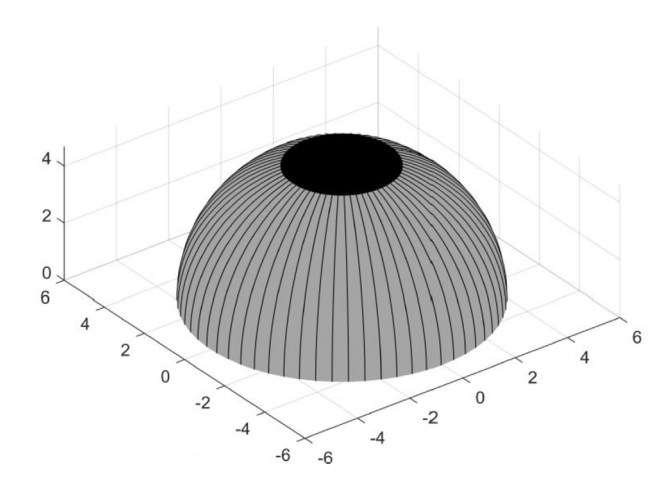


Fig. 1. Schematic of the reference shape of diaphragm.

4. Equilibrium solutions based on a geometric model of diaphragm

In this section, we present a numerical solution of equilibrium equations. The main purpose is to demonstrate the utility of the theoretical model in predicting the shapes and stresses of the diaphragm during inspiration. We choose several values of η and P, and compute the corresponding muscle fiber shortenings and alterations in diaphragm shape and stresses.

4.1. A geometric model

The boundary value problem is based on a geometric model from Amancharla et al. (2001), in which a passive and stress free canine diaphragm is assumed to have an axisymmetric shape, generated by a plane circular curve rotating about the cranial axis. The plane curve corresponds to a muscle fiber from the chest wall insertion to the muscle–tendon junction. The diaphragm in the reference configuration is a hemispherical surface with a central hole, whose dimensions are taken from Amancharla et al. (2001).

We thus take functions \bar{f} and \bar{g} , which define the shape of the passive diaphragm, to be of the form

$$\bar{f}(s) = R\cos\frac{s}{R}, \quad \bar{g}(s) = R\sin\frac{s}{R}, \quad 0 \le s \le L,$$
 (48)

where R is the radius of the circular arc that represents the muscle fiber, which is also the radius of the chest wall into which the muscle fiber is inserted. The central tendon, which is known to be essentially isotropic and inextensible (see Boriek and Rodarte (1997)), is taken as a rigid spherical cap with base radius R_t given by

$$R_t = R\cos\frac{L}{R}. (49$$

A schematic of the passive and stress-free diaphragm is depicted in Fig. 1.

4.2. A boundary value problem

The deformed diaphragm is described by functions f and g which satisfy the equilibrium equations (46) and the kinematic boundary conditions

$$f(0) = R, \quad f(L) = R_t, \quad g(0) = 0.$$
 (50)

The boundary conditions $(50)_{1,3}$ state that the chest wall has no displacement, and $(50)_2$ states that the central tendon has no deformation. Moreover, f and g must also satisfy a traction boundary condition

$$\frac{2g'(L)S_1|_{s=L}}{R_t\sqrt{f'^2(L)+g'^2(L)}} = P,$$
(51)

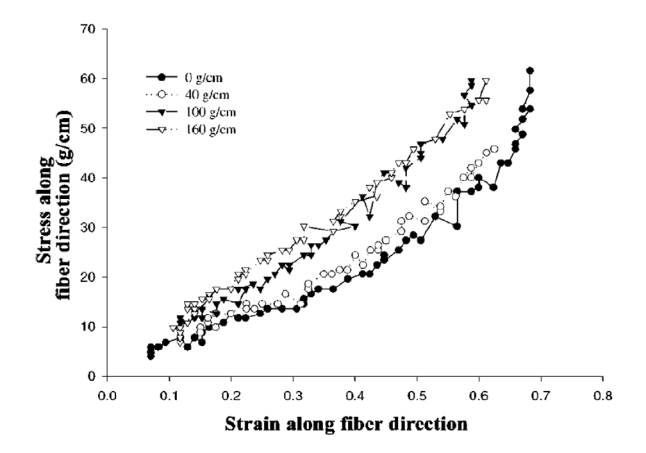


Fig. 2. Stress-strain data under various transverse loads for the passive canine diaphragm in a biaxial experiment by Boriek et al. (2000).

which follows from the force balance of the central tendon. Although the central tendon cannot deform, it can move along the cranial axis e_z , with its displacement given by $g(L) - \bar{g}(L)$.

The constant c in the equilibrium equations (46) can be determined by evaluating the left-hand side of (46)₂ at s = L and using (51), (48)₁, (49), and (50)₂, yielding

$$c = \frac{\bar{f}(L)g'(L)S_1|_{s=L}}{\sqrt{f'^2(L) + g'^2(L)}} - \frac{1}{2}Pf^2(L) = 0.$$
 (52)

Therefore, the equilibrium equations (46) reduce to

$$\left(\frac{Pf^2f'}{2g'}\right)' - S_2(\lambda_1, \lambda_2) + Pfg' = 0, \quad \frac{\bar{f}g'S_1(\lambda_1, \lambda_2)}{\sqrt{f'^2 + g'^2}} - \frac{1}{2}Pf^2 = 0. \quad (53)$$

It is noted that when P=0, the equilibrium equations (53) become algebraic equations

$$S_2(\lambda_1, \lambda_2) = 0, \qquad g'S_1(\lambda_1, \lambda_2) = 0,$$
 (54)

of which the analytical solutions are immediately available. Henceforth, we consider the case where $P \neq 0$.

4.3. Principal stress-principal stretch relations

To find the solutions of the boundary value problem (50) and (53), we utilize the principal stress–principal stretch relations $S_1(\lambda_1, \lambda_2)$ and $S_2(\lambda_1, \lambda_2)$ obtained from curve-fitting the biaxial experimental measurements by Boriek et al. (2000), as shown in Fig. 2. We take the principal stresses to be polynomials of degree 1 in stretches:

$$S_1(\lambda_1,\lambda_2)=a_{11}(\lambda_1-1)+a_{12}(\lambda_2-1), \quad S_2(\lambda_1,\lambda_2)=a_{21}(\lambda_1-1)+a_{22}(\lambda_2-1), \eqno(55)$$

where a_{ij} are constants, which are obtained by fitting the data in Boriek et al. (2000) as

$$a_{11} = 42 \text{ g/cm}, \quad a_{12} = a_{21} = 22 \text{ g/cm}, \quad a_{22} = 73 \text{ g/cm}.$$
 (56)

It is commonly believed that the maximum muscle fiber shortening is about 50%. We thus take $\epsilon=0.5$.

4.4. Solution methods and the results

Our solution strategy is to first covert the equilibrium equations (53) to a system of two nonlinear first-order ordinary differential equations and a nonlinear algebraic equation, and then to use appropriate numerical iteration schemes to solve the system. We introduce two intermediate variables F and G by

$$F(s) = \frac{f'(s)}{g'(s)}, \quad G(s) = g'(s). \tag{57}$$

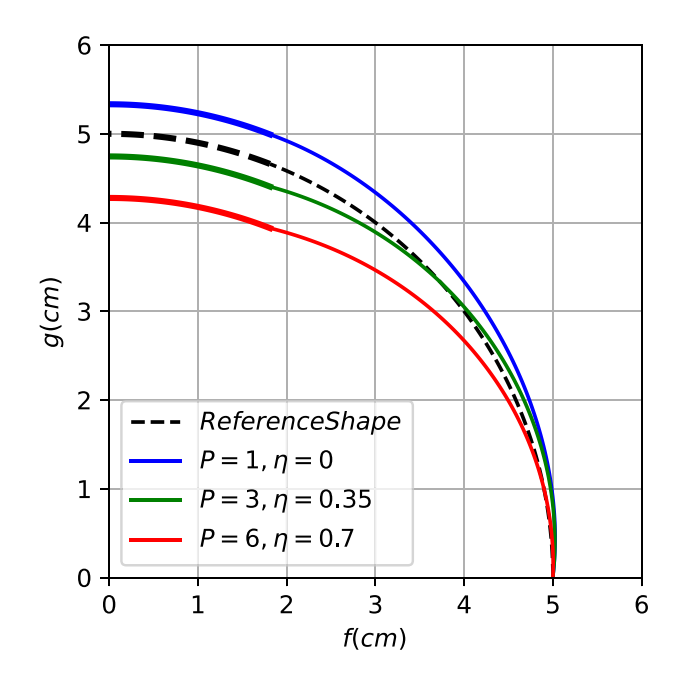


Fig. 3. The shape of diaphragm at various values of the transdiaphragmatic pressure P and the activation parameter η .

Eq. $(53)_2$ can be written as

$$\frac{\bar{f}S_1(\lambda_1, \lambda_2)}{\sqrt{F^2 + 1}} - \frac{1}{2}Pf^2 = 0,$$
(58)

and Eqs. (47) written as

$$\lambda_1 = \frac{G\sqrt{F^2 + 1}}{1 - \epsilon \eta}$$
 and $\lambda_2 = \frac{f}{\bar{f}}$. (59)

Eq. (58) is an algebraic equation for G and can be solved explicitly to yield

$$G = \frac{1 - \epsilon \eta}{\sqrt{F^2 + 1}} \left[1 - \frac{a_{12}}{a_{11}} \left(\frac{f}{\bar{f}} - 1 \right) + \frac{P f^2 \sqrt{F^2 + 1}}{2a_{11}\bar{f}} \right]. \tag{60}$$

Here, we have used $(55)_1$. By (60), (59), and $(55)_2$, we can write Eq. $(53)_1$ as a system of two first-order ordinary differential equations

$$f' = \frac{(1 - \epsilon \eta)F}{\sqrt{F^2 + 1}} \left[1 - \frac{a_{12}}{a_{11}} \left(\frac{f}{\bar{f}} - 1 \right) + \frac{Pf^2 \sqrt{F^2 + 1}}{2a_{11}\bar{f}} \right],$$

$$F' = \frac{2(a_{11}a_{22} - a_{12}a_{21})}{a_{11}Pf^2} \left(\frac{f}{\bar{f}} - 1 \right) + \frac{a_{21}\sqrt{F^2 + 1}}{a_{11}\bar{f}}$$

$$- \frac{2(1 - \epsilon \eta)\sqrt{F^2 + 1}}{f} \left[1 - \frac{a_{12}}{a_{11}} \left(\frac{f}{\bar{f}} - 1 \right) + \frac{Pf^2 \sqrt{F^2 + 1}}{2a_{11}\bar{f}} \right].$$
(61)

The system (61), along with the boundary conditions $(50)_{1,2}$, are solved numerically. Substituting the resulting solution f and F into (60) gives G, which, with $(57)_2$ and the boundary condition $(50)_3$, leads to g.

Functions f and g represent the shape of the diaphragm for prescribed values of the activation parameter η and the transdiaphragmatic pressure P. In Fig. 3, the shapes of the diaphragm are plotted for four combinations of the values of η and P. The thicker portion of each curve corresponds to the central tendon. The reference shape, represented by the dashed curve, corresponds to $\eta=0$ and P=0. The curve with $\eta=0$ and P=1 cmH₂O is the shape of the diaphragm at the beginning of inspiration when the diaphragm is passive and is subject to a baseline transdiaphragmatic pressure. The diaphragm moves up from

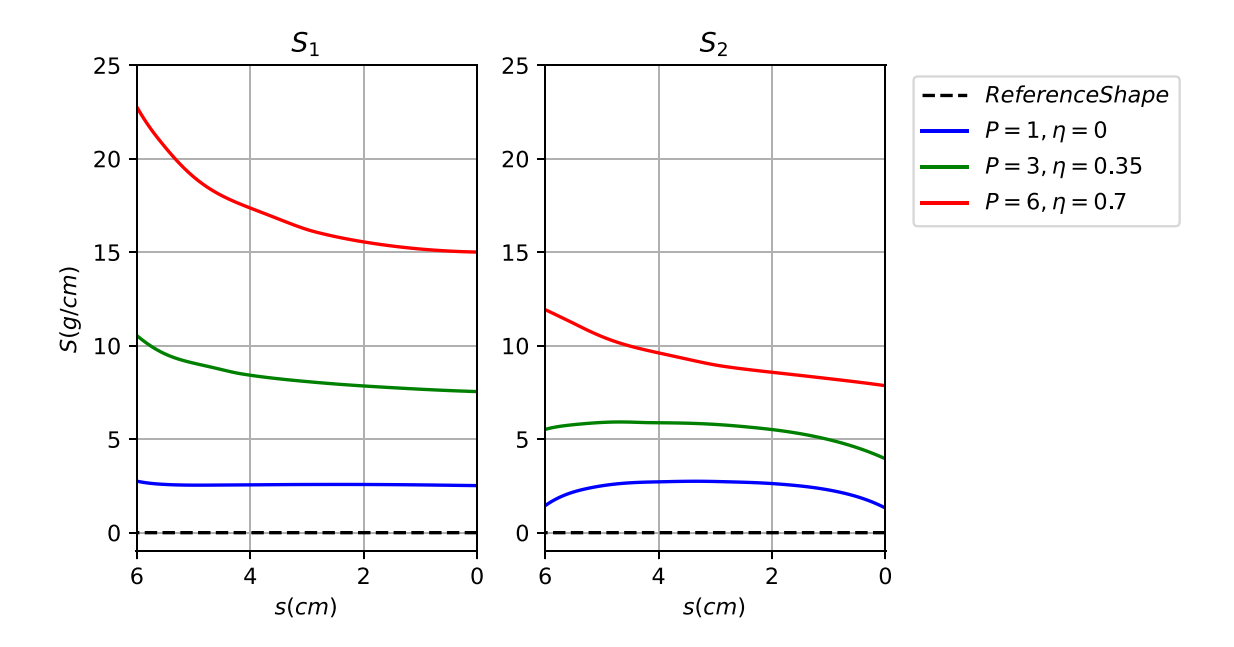


Fig. 4. The distributions of the meridional stress S_1 and the circumferential stress S_2 along the muscle fiber at various values of the transdiaphragmatic pressure P and the activation parameter η .

the reference shape under the action of a positive transdiaphragmatic pressure from the lower side of the diaphragm. The curve with $\eta=0.35$ and P=3 cmH₂O is the shape of the diaphragm in an intermediate state of the inspiration. The increasing transphragmatic pressure tends to move the diaphragm upward, while the activation (shortening) of the muscle fibers tends to move the diaphragm downward. Finally, the curve with $\eta=0.7$ and P=6 cmH₂O is the shape of the diaphragm at a high level of spontaneous muscle activation. The value of the activation parameter 0.7 gives rise to 35% shortening (= $\epsilon\eta$) of the muscle fibers, which agrees with that reported in Amancharla et al. (2001). This muscle fiber shortening causes the diaphragm to move downward, the volume of the thoracic cavity to increase, and the transdiaphragmatic pressure to increase.

For the axisymmetric deformations, the meridional stress S_{11} in the direction of muscle fiber and the circumferential stress S_{22} are identical to $S_1(\lambda_1, \lambda_2)$ and $S_2(\lambda_1, \lambda_2)$, which can be obtained by substituting functions f and g into (47). In Fig. 4, the stresses S_1 and S_2 are plotted along the muscle fiber length s, with s = 0 corresponding to the chest wall insertion and s = 6 cm corresponding to the muscle–tendon junction. The meridional stress S_1 in the muscle fiber direction is seen to increase in the activation parameter η and the transdiaphragmatic pressure P. The stress distribution of S_1 is non-uniform for large values of η and P. At the end of inspiration, the stress at the muscle–tendon junction is about 50% larger than the stress at the chest wall insertion. The value of circumferential stress S_2 , transverse the muscle fiber, is less than the value of S_1 , but also increases in η and P. The stress distribution of S_2 is again non-uniform. However, the transdiaphragmatic pressure P is seen to have an effect of increasing S_2 in the middle portion of the muscle fibers, while the activation parameter η has an effect of increasing S_2 near the muscle-tendon junction.

We note that in these simulations, the value of the transdiaphragmatic pressure P is taken as input of the boundary value problem. The baseline transdiaphragmatic pressure (1 cmH $_2$ O), the intermediate-state pressure (3 cmH $_2$ O), and the high-activation pressure (6 cmH $_2$ O) are estimated from the experimental measurements. In future work, it will be desirable to consider a larger respiratory system that includes the diaphragm, rib cage, lungs, bronchial tubes, throat, nose, and mouth, and to determine the transdiaphragmatic pressure as a part of

the solution to a large system of governing equations for the respiratory system.

5. Summary

A theoretical framework for mechanics of diaphragm is developed. The salient features include:

- The diaphragm is modeled as an active anisotropic elastic material surface. This material surface model allows for analytical determination of the diaphragm shape and the stress distributions with high accuracies and minimum computational efforts.
- A constitutive theory for diaphragm is developed which incorporates the activation mechanism of the skeletal muscle fibers. The resulting constitutive function gives the stress-strain relations of the diaphragm in the entire range of activations, from the passive state to the maximum activation state.
- The anisotropy due to the muscle fibers is fully embodied in the constitutive theory.
- The equilibrium equations are derived that are partial differential equations for the deformation of the diaphragm.
- The equilibrium equations reduce to ordinary differential equations for axisymmetric deformations, which can be readily solved numerically. Furthermore, only partial information of the constitutive functions, which can be obtained from the existing biaxial experiments, is needed for such solutions.
- A complete boundary value problem is formulated. The solutions enable determinations and predictions of the diaphragm shapes, stress distributions, and volume displacements in the full range of the respiration process.

Future investigations may include refinements of the constitutive models, development of new experiments to determine the complete constitutive function and the activation function, and development of the solution methods for more realistic geometric models and non-axisymmetric deformations. A fully developed model will provide the researchers and clinicians with powerful analytic tools to conduct patient-specific studies of the respiratory system, and thus empowers them to undertake the tasks that are not previously possible.

CRediT authorship contribution statement

Yi-chao Chen: Conceptualization, Investigation, Formal analysis, Writing – review & editing, Writing – original draft, Methodology. **Aladin M. Boriek:** Writing – original draft, Methodology, Investigation, Formal analysis, Data curation, Conceptualization.

Declaration of competing interest

The authors declare that they have no known competing financial interests or personal relationships that could have appeared to influence the work reported in this paper.

Acknowledgments

The authors wish to acknowledge My Alhassan's assistance in carrying out the numerical analysis to solve the equilibrium equations. This work was supported partly by the National Science Foundation, United States of America Grant 1714478.

References

- Amancharla, M.R., Rodarte, J.R., Boriek, A.M., 2001. Modeling the kinematics of the canine midcostal diaphragm. Am. J. Plysiol. Regul. Intetr. Comp. Physiol. 280, 588–597
- Boriek, A.M., Hwang, W., Trinh, L., Rodarte, J.R., 2005. Shape and tension distribution of the active canine diaphragm. Am. J. Physiol. Regul. Intetr. Comp. Physiol. 288, 1021–1027.
- Boriek, A.M., Kelly, N.G., Rodarte, J.R., Wilson, T.A., 2000. Biaxial constitutive relations for the passive canine diaphragm. J. Appl. Physiol. 89, 2187–2190.
- Boriek, A.M., Rodarte, J.R., 1997. Effects of transverse fiber stiffness and central tendon on displacement and shape of a simple diaphragm model. J. Appl. Physiol. 82, 1626–1636
- Fung, Y.C., 1981. Biomechanics Mechanical Properties of Living Tissues. Springer,
- Greybeck, B.J., Wettergreen, M., Hubmayr, R.D., Amancharla, M.R., Boriek, A.M., 2011.
 Diaphragm curvature modulates the relationship between muscle shortening and volume displacement. Am. J. Physiol. Regul. Intetr. Comp. Physiol. 301, 76–82.
- Kim, J.A., Druz, W.S., Danon, J., Machnach, W., Sharp, J.T., 1976. Mechanics of the canine diaphragm. J. Appl. Physiol. 41, 369–382.
- Ogden, R.W., 1984. Non-Linear Elastic Deformations. Ellis Horwood.
- Strumpt, R.K., Humphrey, J.D., Yin, F.C.P., 1993. Biaxial mechanical properties of passive and tetanized canine diaphragm. Am. J. Physiol. 265, 469–475.